Phosphoproteomics identifies PI3K inhibitor-selective adaptive responses in pancreatic cancer cell therapy and resistance

Short title: Mapping PI3K inhibitor-dependent phosphoproteome

Cintas C[1,2], Douche T[1,2], Dantes Z[3], Mouton-Barbosa E[4], Bousquet MP[4], Therville N[1,2], Pont F[1], Cayron C[1,2], Ramos-Delgado F[1,2], Thibault B[1,2], Garmy-Susini B[5], Cappello P[6], Burlet-Schiltz O[4], Hirsch E[6], Gomez-Brouchet A[7], Reichert M[3], Guillermet-Guibert J[1,2].

[1] INSERM U1037, CRCT, Université Paul Sabatier, Toulouse, France

[2] Labex TouCAN, Toulouse, France

[3] TUM Technical University of Munich, Germany

[4] Institut de Pharmacologie et de Biologie Structurale (IPBS), Université de Toulouse, CNRS UMR 5089, UPS, Toulouse, France

[5] I2MC, INSERM U858, Université Paul Sabatier, Toulouse, France

[6] MBC, Turino, Italy

[7] IUCT-O, Biobank, Toulouse, France

The authors do not have conflicts of interest.

Abstract

236 words (max 250 words)

The PI3K pathway is highly active in human cancers. The four class I isoforms of PI3K are activated by distinct mechanisms leading to a common downstream signaling. Their downstream redundancy is thought to be responsible for treatment failures of PI3K inhibitors. We challenged this concept, by mapping the differential phosphoproteome evolution in response to PI3K inhibitors with different isoform selectivity patterns in pancreatic cancer, a disease currently without effective therapy. In pancreatic cancer, PI3K signal was shown to control cell proliferation. We compared the effects of LY294002 that inhibit with equal potency all class I isoenzymes and downstream mTOR with the action of inhibitors with higher isoform-selectivity towards PI3Kα, PI3Kβ or PI3Kγ (namely A66, TGX-221 and AS-252424). A bioinformatics global pathway analysis of phosphoproteomics data allowed us to identify common and specific signals activated by PI3K inhibitors supported by the biological data. AS-252424 was the most effective treatment and induced apoptotic pathway activation as well as the highest changes in global phosphorylation-regulated cell signal. However, AS-252424 treatment induced re-activation of Akt, therefore decreasing the treatment outcome on cell survival. Reversely, AS-252424 and A66 combination treatment prevented p-Akt reactivation and led to synergistic action in cell lines and patient organoids. This work paves the road to demonstrate that there are unique adaptive signaling responses to isoform-selective PI3K inhibition. Mapping PI3K isoform pathways will help to design better combinative treatments that prevent the induction of selective compensatory signals.

Graphical abstract

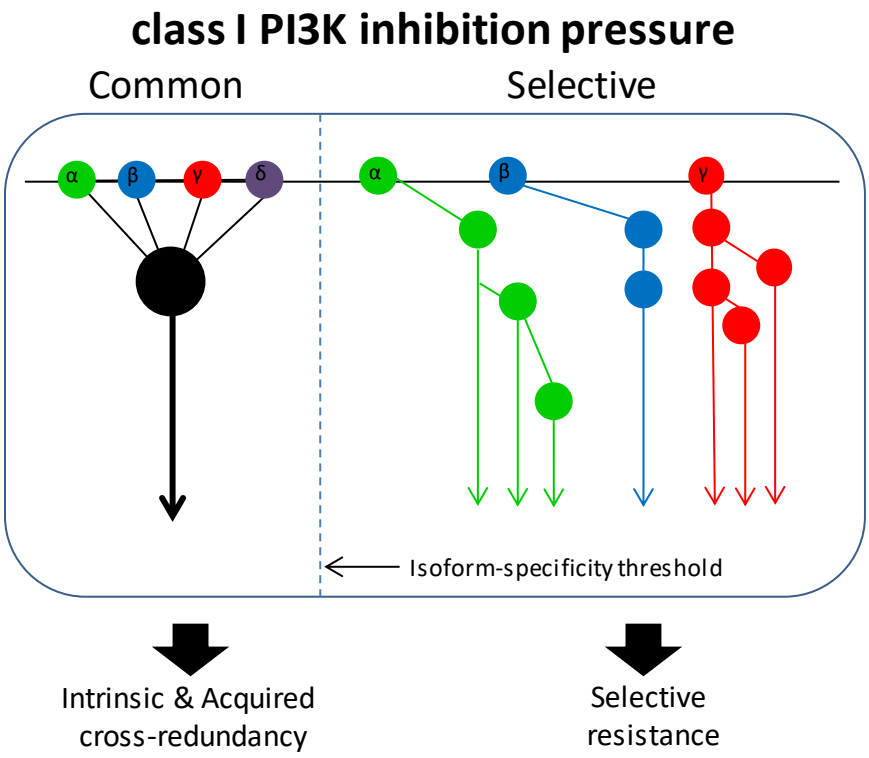

Significance

Half of all human cancers show increased PI3K activity but the mutational pattern of the PI3K pathway is not sufficient to predict sensitivity to PI3K inhibitors. By identifying for the first time specific signaling induced by PI3K inhibitors with different isoform-selectivity patterns, we provide insight in how to handle heterogeneity of PI3K expression in tumor samples for the choice of available PI3K-targetting drugs. Our work provides a roadmap to target the PI3K pathway, balancing the use of isoform-selective PI3K inhibitors with personalized information extending beyond the specific mutational status.

(4874 words)

Introduction

In pathophysiological signaling, biochemical and biomechanical cues are integrated and regulated at long-term. Similarly, it is expected that inhibition of signaling pathways by targeted therapies towards one signal transduction enzyme also induces an adaptation of the entire signaling network that depends on the environmental context.

Class I PI3Ks are crucial signal transduction enzymes. Across species, the dogma for their involvement in cell signaling is the following: after acute stimulation, PI3K phosphorylates the lipid second messenger phosphatidylinositol 4,5-biphosphate into PI-3,4,5-triphosphate (PIP_3) at the plasma membrane, further activating the protein kinases Akt and mTOR, and regulating major cell biology events such as cell proliferation, cell survival and protein synthesis. PI3K is one of the most altered pathways in cancers, and presents 4 different isoforms encoded by 4 different genes (*1*, *2*). Due to the regulation of fundamental cellular processes by PI3K/Akt/mTOR, this signaling axis is an excellent therapeutic target in cancer which is underscored by the number of molecules tested currently in clinical trials (*3*). While class I PI3K isoform specificity is well described and accepted in physiology (for review: (*1*), examples: (*4*–*7*)), potential benefits of isoform-selective targeting in solid cancer were recently shown in breast cancers driven by oncogenic PI3Kα (*8*) but are still not yet approved in other genetic context promoting PI3K signaling (*3*). Besides, there are other effectors downstream PI3Ks than Akt/mTOR (*9*, *10*). Such other downstream signaling routes and feedback loops are possibly contributing to the isoform-specific *in vivo* role of mammalian PI3Ks. Although acquired cross-activation mechanisms between PI3K isoforms upon their unique and selective pharmacological or genetic inhibition in the context of specific mutational landscapes (e.g. oncogenic *PIK3CA*, mutant *PTEN*) has been described (*11*–*13*), a specific large scale signal transduction and cell adaptation to such treatment is unknown, in particular, in the context of non-mutated PI3Ks and/or Kras mutation. This genetic context is found in pancreatic ductal adenocarcinoma (PDAC). Importantly, it is also unclear whether differing inhibition of each

PI3K due to distinct PI3K inhibitor selectivity or due to different isoform expression could favor selective feedback mechanisms; the latter could be an unprecedented explanation of the therapeutic failure of PI3K inhibitors in unselected solid tumours.

New strategies are needed for the cure of pancreatic cancer (PDAC) patients, due to dramatic lethality rate of this disease. PI3K signaling as assessed by Akt phosphorylation or by PI3K/Akt/mTOR gene signature is increased and associated with poor prognosis in patients who underwent surgery (*14*, *15*). This increase in PI3K signaling is mostly due to Kras mutation engaging PI3Kα and possibly PI3Kγ (*16–19*). PI3K signaling downstream Kras is amplified by other signaling cues (*20*) and such amplification of Kras-PI3K coupling is critically involved in PDAC poor prognosis (*21*). Targeting PI3K is expected to have a clinical action in these patients (clinical trials pending as reviewed in (*22*) and (*23*)). However, prior knowledge of cancer cell adaptation to the inhibition of upstream class I PI3K signaling would be necessary to develop efficient anti-PI3K therapeutic strategy in cancer and in particular in pancreatic disease. The concentration of selective inhibitors used in patients is largely higher than the IC_{50} of the inhibitors *in vitro* (*8*) and their isoform specificity, emphasizing possible off-target or redundancy effects in patients. Understanding of adaptive processes upon treatment with inhibitors could impact the design of combination therapy (*22*). The purpose of the study is to compare the pancreatic cancer cell phosphoproteome in response to inhibitors with different selectivity and off-targets profiles, as an exploratory experiment to find first evidence of isoform selective pathways and adaptive responses.

Therefore, we analyzed adaptive signals involved in response to inhibitors with distinct PI3K-isoform selectivity in a human pancreatic cell line using a stable isotope labeling with amino acids in cell culture (SILAC)-based quantitative phosphoproteomics approach in a comprehensive way. By enrichment of the phosphoproteome followed by data mining, we demonstrate that, despite a common core pathway regulated by all inhibitors, the different PI3K inhibitors instruct specific, non-redundant signaling pathways linked to PI3K signaling. These data might help to better design therapeutic strategies in this dismal disease.

Results

PI3K inhibitors induce different adaptive phospho-proteome responses in pancreatic cancer

In pancreatic cancer, PI3K signaling is associated with a poor prognosis (*14*, *15*). The analysis of 11 pancreatic cancer samples compared to normal adjacent tissue showed increase Akt expression and a significant increase of S473 and T308 Akt phosphorylation by western blot (WB) (9 out of 11 patients) (**Figure 1A**, **Supplementary Figure 1A**). However, the observed increase of Akt phosphorylation was not always associated with a significant increase in the phosphorylation levels of canonical downstream targets, such as pPRAS40 or pS6K (**Figure 1A, right**), emphasizing the heterogeneity of signaling targets downstream PI3Ks in a clinical setting.

The human pancreatic cancer cell line Capan-1 represents common genetic alterations found in PDAC including *KRAS, TP53 and SMAD4* mutations (*24*), expresses all four PI3K isoforms (*16*, *25*) and displays a proliferation rate similar to other human pancreatic cell lines (as verified in **Supplementary Figure 1B**). Amongst the four PI3K isoforms responsible for the production of PIP_3 and Akt activation, we and others have identified PI3Kα and PI3Kγ to be involved in pancreatic carcinogenesis (*16*, *17*, *26–28*). Besides oncogenic Kras-driven activation of PI3K (*20*), stimulation by fetal bovine serum (FBS) induces the activation of receptor tyrosine kinases (RTKs) and G protein-coupled receptors (GPCRs) that increases pAkt level (*7*). Short-term (10min) FBS stimulation induced a significant activation of class I PI3Ks as assessed by the phosphorylation of Akt and a known downstream effector, PRAS40 (**Figure 1B**). We used a pan-PI3K/mTOR-targeting inhibitor that inhibits all PI3K isoforms at equal potency [LY-294002 from here on named pan-inh]. Pan-inh completely abolished pAkt and pPRAS40 (**Figure 1B**). Isoform-selective drugs targeting either PI3Kα (A66 [5μM], α-inh (*29*)), PI3Kβ (TGX-221 [0.5μM], β-inh (*7*, *30*)) and PI3Kγ (AS-252424 [5μM], γ-inh (*31*)), but not of PI3Kδ inhibitor (IC-87114 [5μM], δ-inh), inhibited pS473Akt as well as pPRAS40 levels significantly after 10min of FBS-stimulation (**Figure 1B**). PI3K inhibitors are still effective to

inhibit pAkt when diluted in cell medium 24h prior to treatment *in vitro* demonstrating the stability of the compounds at long-term (**Supplementary Figure 1C**).

To explore the possibility of isoform-selective downstream pathways, we devised an exploratory strategy to identify adaptive response to PI3K inhibitors with varying selectivity and off-targets effects in a comprehensive fashion by defining phospho-site regulated signaling pathways in Capan-1 cell line (**Figure 1C**). To quantify subtle differences between these conditions targeting the same enzymatic activity, we chose a SILAC-based quantitative approach combined to a phospho-peptide enrichment by TiO2 allowing a robust S/T/Y phosphorylation quantification of thousands of proteins. We devised a super-SILAC approach (*32*, *33*), in which we compared all the unlabeled treatment conditions to vehicle control, with the use of SILAC-labeled cells as a spike-in standard for accurate quantification of unlabeled samples (**Figure 1C, Supplementary Table 1**). Incorporation of heavy isotopes was verified by mass spectrometry after 6 passages (**Supplementary Figures 2A, 2B**); and the metabolic labelling did not change the proliferation and morphological properties of Capan-1 cell line (**Supplementary Figures 2C, 2D**). All validating steps are detailed in **Supplemental Material & Methods** and **Supplementary Figures 2**. In all conditions combined, 3600 heavy/light phospho-peptides were detected and quantified (**Figure 1C**). Amongst these, 83% serine-sites (S), 16% threonine-sites (T), 1% tyrosine-sites (Y) were phosphorylated (**Supplementary Figure 2F**). These percentages were unchanged upon PI3K inhibition (**Supplementary Figure 2G**). Short-term (10min)- and long-term (24h)-serum stimulation induced modifications (increased and decreased) of 557 phospho-peptides (28%) and 619 phospho-peptides (32%), respectively (**Supplementary Figures 2H, 2I**).

Overall, levels of a known PI3K target PRAS40 were changed in similar manner albeit with a slight lower dynamic range when quantified by MS-based proteomics analysis compared to western blot results (**Supplementary Figures 2J** vs. **Figure 1B**).

We next identified phospho-peptides with significant altered levels in each condition in an unbiased fashion. PI3K inhibitors induced more phosphorylation level changes after 24h of treatment than after 10min. Interestingly, γ-inh led to the most significant changes in phosphoproteome compared to FBS as soon as 10min of treatment, and global equivalent phosphoprotein level changes at 24h compared to α-inh (**Figure 1D**). These strong phosphoprotein modulations by γ-inh and α-inh after 24h of treatment suggest signaling engagement of these two PI3K isoforms in PDAC cells, in addition to their involvement in pancreatic carcinogenesis.

The number of significantly increased p-peptides in γ-inh condition (and to slighter extent of pan-inh) was higher at short time compared to α-inh but decreased at 24h, possibly suggesting an early induction of feedback control with these two PI3K inhibitors. Reversely, α-inh treatment led to increased p-peptides at 24h. β-inh treatment led to a balanced increase/decrease of p-peptides at both times (**Figure 1D**). Early upregulated signaling are expected to reduce the efficiency of PI3Kγ inhibitors.

Global pathway analysis of phosphoproteome upon PI3K inhibition shows selective changes associated with different isoform-specificity

We next analyzed dynamic changes in the phosphoproteome upon PI3K isoform-specific inhibition over time (10min vs. 24h treatment) using global pathway analysis 1- to identify selectivity in regulating biological functions by each inhibitor, and 2- visualize entire signal network rewiring upon PI3K inhibition pressure.

A principal component analysis (PCA) of the phosphoproteome at 10min demonstrated that serum-stimulation alone, α-inh and β-inh conditions clustered together while pan-inh and γ-inh conditions separated from the cluster (**Figure 2A, left**). After 24h of treatment, however, all inhibitor treatments separated from the FBS condition, highlighting the time necessary to induce significant PI3K inhibitor-selective changes in signaling networks upon PI3K inhibition, particularly for PI3K isoform-specific inhibition (**Figure 2A, right**). Surprisingly, inhibition with

LY (pan-inh) clustered closely together with the β-inh, while γ- and α-inh conditions led to distinct phosphopeptide modifications, in line with the known selective roles of these isoforms in PDAC (*17*, *25*, *26*).

Next, we identified inhibitor-selectivity in regulated phosphoproteomes at both time points using hierarchical clustering (**Supplemental Material and Methods, Supplementary Table 1, 2, 3**). By overlapping phosphopeptides with altered levels in each condition, we were able to identify shared (core) phosphopeptides, inhibitor-selective phosphopeptides indicated as either A66-selective (α-inh -select), TGX-221-selective (β-inh -select) or AS252424 -selective (γ-inh select), as well as pan/mTOR-selective (pan-inh-select) phosphopeptides (**Figures 2B, 2C, Supplementary Figure 3**). The finding that there is a common "core" of phosphopeptides regulated by all PI3K inhibitors was underscored by STRING analyses of inhibitor-selective and common phosphopeptides **(Supplementary Figures 3A, 3B, Supplementary Table 1, 2, 3**). This core network presented a strong connectivity in particular at 10min of treatment.

Our data also demonstrate that each inhibitor induced distinct changes of the phosphorylation-regulated proteome already at 10min of treatment (**Figure 2A, 2B)**, despite having similar effects on the phosphorylation of Akt and PRAS40 (**Figure 1B**). Inhibitor-selective as well as core phosphopeptides showed distinct pathway enrichments (Reactome), cellular components and molecular functions (Gene Ontology) at the 10min and 24h time points (**Figure 2C, Supplementary Figure 3**). At 10min, common core downstream signaling include 115 phosphoproteins implicated in mRNA splicing, chromatin regulation, TGFβ signaling as well as gene transcription and transcript processing pathways (ZE Pvalue ≤0.05) (**Figures 2C**). Interestingly, at 24h, γ-inh-selective phosphopeptides were enriched in similar functions and cellular components as those changed by all PI3Ks/mTOR (core and pan-inh select), with targets presenting a strong protein-protein interactivity (**Figure 2C, Supplementary Figures 3F-J**). Apart from the core pathways, α-inh-selective and β-inh-selective phosphopeptides were enriched in different pathways at both time points. Specifically, α-inh modulated phosphopeptides regulating RTK and cytokine signaling,

whereas β-inh regulated phosphopeptides directing mitotic control (**Figure 2C, Supplementary 3D, E,G-J**).

To estimate on-target and off-target effects of inhibitors, we used STRING connectivity analysis and showed that inhibitor selective targets were associated and connected with PI3K isoforms, except for TGX-221 treatment at 24h **(Supplementary Figures 3E, Supplementary Table 1, 2, 3**). The proteins involved were either off-targets of TGX-221 (β-inh) or were unknown targets of PI3Kβ. These data show that PI3K inhibition with AS252424 (γ-inh) regulates similar processes to pan-inh and, at the same time, controls additional core networks exceeding the effect of pan-inh on signal network as shown by the number of non-selective and selective phosphopeptides modified by γ-inh treatment (**Figure 2B**).

These findings suggest that inhibiting strongly PI3Kγ might be the most effective therapeutic strategy in this cell line to inhibit the core PI3K signaling in order to target essential growth and survival pathways in pancreatic cancer.

Pancreatic cancer cells present increased levels of p110γ expression in patients

We next analyzed the expression levels of PI3K catalytic subunits that constitute the four class I isoforms (α, β, γ and δ) in tumor cell-enriched human pancreatic cancer samples compared to normal adjacent pancreas by Western Blot. We observed that p110β levels were increased only in 5 patients, while p110α, p110γ and p110δ protein levels were significantly increased (in all but one patient) (**Figure 3A**). To further verify these findings in a pure population of cancer cells, we analyzed PI3K isoforms protein and mRNA levels in human (n=4) and murine (n=7) cell lines (derived from genetically modified mouse models of PDAC) (**Figure 3B-E**). The myeloid cell line, MOLM-14, which is known to express p110γ in high abundancy served as positive control.

In contrast to tumor cell-enriched human pancreatic cancer samples, p110γ was only found detected in one out of four human pancreatic cancer cell lines and in two out of seven murine pancreatic cancer cell lines by WB (**Figure 3B, 3C**). Similarly, on a transcript level, two out of four human PDAC cell lines and three out of seven murine PDAC cell lines showed increase

in p110γ mRNA expression by RT-qPCR (**Figure 3D, 3E)**. This data indicates that p110γ is overexpressed in patient-derived tumor cell-enriched PDAC samples and to a lesser extent in PDAC cells *in vitro,* questioning the tumor-intrinsic role of p110γ.

Pancreatic cancer cells are sensitive to PI3Kγ inhibition *in vitro* and *in vivo*

We next confirmed that genetic inactivation of PI3Kγ using a full knock-out approach almost completely abolished cancer formation from precancer lesions (PanIN) in a mutated KRAS and p53 background (**Figure 4A**)**.** Similarly, despite the low expression levels of p110γ *in vitro*, decreased expression of p110γ using a shRNA approach reduced the clonogenicity of Capan-1 cell line (**Figure 4B**). Of note, we did observe decreased PI3Kα expression upon p110γ knockdown by shRNA in one pool of cells, but that led to similar effects that the other shp110γ pool of cells.

We tested isoform-selective inhibitors on a panel of Human pancreatic cancer cells lines. γ-inh significantly decreased pAkt at 10min in the four cell lines (**Figure 4C, Supplementary Figure 4A**). These experiments aimed to validate the pathway analysis on inhibitor-selective phosphoproteome, by comparing with experimental cellular outputs.

β-inh led to increased cell numbers in Capan-1 cells only (**Figure 4D**). BxPC-3 cells (non-mutated *KRAS* cell line) was sensitive to all tested inhibitors (**Figure 4D**). Cell numbers of all human pancreatic cancer cell lines were significantly decreased in time upon γ-inh or pan-inh as compared to vehicle, regardless p110γ mRNA level of expression, while α-inh was efficient only in BxPC-3 and Panc-1 cell lines (**Figure 4D**). γ-inh was almost as effective or more effective (Capan-1) that pan-inh. This was confirmed with BrdU incorporation assay, cell cycle analysis and cleaved caspase-3 analysis (**Supplementary Figure 4B-D)**. Interestingly, only γ-inh treatment induced significant increase of DEVDase activity (**Supplementary Figure 4D**), confirming the selective enrichment of the “Apoptotic cleavage of cellular proteins” signaling pathway by γ-inh (**Figure 2C right**).

Long-term inhibition of PI3Kγ allows compensation between PI3K isoforms in pancreatic cancer

We next analyzed the activation of PI3K canonical pathway at 24h. In Capan-1 cells, 24h inhibition with pan-inh or γ-inh led to a re-activation of p-Akt (**Figure 5A**)**.** α-inh treatment did not show such upregulation of pAkt, in the four tested cell lines (**Figure 5A**). The combination of α-inh and γ-inh prevented this reactivation at 24h compared to γ-inh treatment. The re-activation of pAkt upon γ-inh or pan-inh treatment was observed in 3 and 2 out of 4 cell lines, respectively (**Figure 5A, Supplementary Figure 4A**).

Interestingly, if we were able to identify selectively changed phosphopeptides in all conditions tested, pan-inh or γ-inh conditions also led to the identification of higher numbers of selective phosphoproteins (**Figure 2B**), that are known to be inter-regulated (**Supplementary Figure 3B, 3C, 3F**), and leading similar pathway enrichments (**Figure 2C**). This could also correspond to the induction of negative feedback loops. Indeed, Kinase Enrichment Analysis showed that pan-inh and γ-inh treatment induced the phosphorylation of peptides that corresponds to RPS6KB2 (S6K2) kinase motif ($p<0.05$) and to MAPK9 with lower statistical power (**Supplementary Figure 5**). These bioinformatic data are line with the observed re-induction of pAkt upon pan-inh or γ-inh treatments (**Figure 5A**).

Analysis of phosphopeptides regulated selectively by PI3Kα inhibitor at 24h in **Figure 2C** and in **Supplementary Figure 3D** showed that PI3Kα regulated additional functions and cellular components compared to panPI3K/mTOR or PI3Kγ-selective phosphopeptides. We thus tested the combination of α-inh and γ-inh on cell survival and showed that this combination led to a higher efficiency than each inhibitor alone or than PI3K/mTOR inhibitor in three out of four cell lines (**Supplementary Figure 6**). The only cell line (MIA Paca-2) where the combination was not more effective on cell survival was the one where we did not detect a feedback loop on pAkt upon PI3K inhibition. Combination of γ-inh with other isoform PI3Kβ or PI3Kδ inhibitors appeared to be less synergistic (**Supplementary Figure 6**). This corroborates

the phosphoproteomic analysis that identifies feedback mechanisms on S6K upon PI3Kγ inhibition.

We next asked the question if the phosphopeptides selectively regulated at long-term by either PI3Kα or PI3Kγ inhibitors correlate with the effect of each PI3K inhibitor. The changes in ratios of pGIGYF2 (T382) correlated with PI3K action on pancreatic cell survival/proliferation (**Supplementary Figure 7A,** WO2019101871-A1). Interestingly, changes of phosphorylation levels of known targets of PI3K as assessed by WB (**Supplementary Figure 4A**) did not correlated with the cellular action in the four pancreatic cancer cell lines (**Supplementary Figure 7B**).

The combination of PI3Kα and PI3Kγ selective inhibitors is synergistic in PDAC patients.

Finally, we aimed to test this synergy in a clinically relevant setting, in two pancreatic cancer patient-derived organoids (PDOs) (B25 and B34) that displayed representative genetic alterations and p110s expression (**Figure 5B, 5C**). Here, we observed that the equimolar combination of PI3Kα-inh and PI3Kγ-inh led to an increased sensitivity to PI3K inhibition as assessed with the metabolism measurements of organoids (**Figures 5D, 5E**). In cell lines and PDOs tested, combined treatment had additive (2/6) or synergistic effect (4/6 including the two PDOs) at high concentration (5µM) (**Figure 5F, Supplementary Figure 8**). At lower concentration (500nM), combination was antagonistic for the cell lines except for the non-mutant KRAS cell line BxPC-3 and the PDO B34.

Overall, we observed a good correlation between the global phosphorylation-regulated pathway analysis and measured cellular effects upon PI3K inhibitor-selective pressure, providing the first evidence of isoform-selective downstream pathways. These data also suggest that complete inhibition of PI3K with strong efficiency on PI3Kα and PI3Kγ is the most effective strategy for pancreatic cancer patients (WO2019073031-A1). This specific

combination suppresses PI3K/Akt pathway in long-term manner, decreases efficiently cell survival and prevents tumor cell adaptation to PI3K signal blockage.

Discussion

Whether critical signal nodes can be circumvented is a fundamental question in tumoral biology and therapy resistance. Using a phosphoproteomics screen, we demonstrate that each PI3K inhibitor with distinct isoform selectivity displays differential effects on the phosphoproteome of pancreatic cancer cells. Reciprocal class I PI3K signaling is the exclusive product of inhibition-imposed pressure. Accordingly, a selective and strong inhibition of PI3K isoforms is able to induce selective pathway rewiring which could facilitate selective resistance (**Graphical abstract**).

Preclinical data in pancreatic cancer have indicated for a long time that PI3K could be a suitable target in PDAC patients (initial study using Wortmannin in xenografts of Human pancreatic cancer cell lines (*34*)). There is now an urgent need to prevent feedback loops involved in pancreatic cancer progression upon pan-PI3K treatment. One strategy consists of identifying tumors which are more likely to respond. Indeed, it was recently shown that *p27kip1*, encoding a cyclin-dependent kinase inhibitor, facilitated NVP-BEZ235 (PI3K/mTOR inhibitor) sensitivity in a gene dose dependent fashion and knockdown of *p27kip1* decreased NVP-BEZ235 response in murine PDAC cell lines (*35*).

We propose that, further to MAPK signaling (*36–38*), adaptive response to PI3K inhibition also unleash compensatory inter-isoform selective signaling that is dependent on the isoform-selectivity of the inhibitor; this could be circumvented by well-balanced isoforms specific PI3K inhibitors. Given our results so far obtained with the first generation of isoform-selective PI3K inhibitors, we are convinced that the clinically approved Alpelisib/BYL-719 (*8*) combined with IPI-549 (*27*) should be tested in the future in vitro, in preclinical and clinical studies of PDAC.

Us and others have mostly described: either 1- immediate compensations/redundancy between isoforms that are activated through similar mechanisms (e.g. PI3Kα and PI3Kδ downstream RTK (*39*); or PI3Kγ and PI3Kβ downstream GPCR (*7*)), or 2- delayed (in 1-2 week

time) compensation/redundancy between the two ubiquitously expressed PI3K, PI3Kα and PI3Kβ, via genetic induction of their selective of mode activation (e.g. overexpression of RTK, mutation of PTEN) (*11*, *12*, *40*). We identify here a possible novel mode of resistance, which is based on rapid rewiring network. Next study will need to confirm that it is isoform-selective and not inhibitor-selective as well as dissect the possible mechanisms of signal rewiring. It thus remains to be demonstrated that level and duration of activation of downstream effectors including those of Akt, but also global signal rewiring could be isoform-selective.

Given the fact that PI3Kγ and PI3Kβ isoforms are both downstream of GPCRs (*7*), we were surprised to observe that PI3Kγ and PI3Kβ inactivation did not lead to similar phosphoproteomic profiles, nor to similar alteration of cellular functions. One explanation of the poor effect of TGX-221 on these cells despite the observed reduced p-Akt levels could be the concomitant increased number of significantly increased p-peptides.

Of note, based on our results, isoform cross-compensation (in a context of non-mutated PI3K or of no loss of PTEN and of KRAS-mutant or not) appears to involve PI3Kα and the lowly expressed PI3Kγ. Because low level of expression of p110s could be difficult to detect, our data show the importance of determining the level of activation of each class I PI3K possibly with isoform selective gene signatures representative of their activity (*41*). It is also surprising that despite PI3Kγ having low levels of expression, its selective inhibition in serum-deprived condition was effective in all tested cell lines as others reported (*26*, *42*). Importantly, the level of an identified PI3Kγ-selective phosphopeptide (phopho-GIGYG2 T382) was correlated with PI3K sensitivity. We hence propose that the level of phosphorylation of this selective target could be tested as a predictive marker of sensitivity, attesting the induction of selective compensation and efficiency of combinatory treatment with PI3Kα and PI3Kγ inhibitors.

Specific engagement of either PI3Kα or PI3Kγ downstream different types of Kras mutations was recently described (*18*, *19*). It is also interesting to note that the synergistic effect of the tested combination was found in the mutated Kras cell lines, and that the PDO with increased frequence of Kras allele mutations (B34) displayed an increased combination index. These

intriguing data prompt the better delineation of PI3Kα and PI3Kγ possible cooperation in various Kras-mutant contexts.

So far, only multi-combinatorial therapies displayed positive clinical outcome for PDAC patients (*22*). Isoform-specific drugs are expected to induce fewer secondary effects (*3*) and could thus be included in these multi-drug combinatorial therapies. As we show that selective inhibitors at high doses induce selective feedback and resistance mechanism (**Graphical abstract**), these can be counteracted with the increasing arsenal of PI3K isoform-selective agents that are available for clinical use, in particular with Alpelisib and IPI-549 (*8*, *27*). In sum, results shown here highlight that defining pharmacological profiles that are well-balanced towards each class I PI3K isoforms is key to therapeutic success.

Material and Methods

Reagents

Reagents were purchased as follows: pan-PI3K and isoform-selective PI3K inhibitors from Axon Medchem; Gemcitabine was a kind gift of hospital (IUCT-O, France); MTT was from Euromedex (4022). All PI3K inhibitors were resuspended in DMSO, corresponding at the vehicle condition. All products were resuspended according to the supplier's instructions. For all experiments, except for the dose-response experiments, PI3K inhibitors were used at 10µM for LY-294002 (pan-inh), 5µM for A66 (PI3Kα inhibitor named α-inh), 500nM for TGX-221 (PI3Kβ inhibitor named β-inh), 5µM for AS-252424 (PI3Kγ inhibitor named γ-inh) and 5µM for IC-87114 (PI3Kδ inhibitor named δ-inh).

Cell lines and tissue samples

Human pancreatic cell lines (Capan-1, BxPC-3, PANC-1, MIA PaCa-2) came from American Type Culture Collection (ATCC), human acute myeloid leukemia cell line (MOLM4) and murine pancreatic cancer cell lines (DT4994, DT6585, DT6606, DT8442, DT8661, R221, R259) were made in house or a kind gift from Dieter Saur (Klinikum rechts der Isar der TU München,

Germany); for validation of genotype (*16*). Absence of mycoplasma contamination was verified periodically by PCR. Tumor samples to generate pancreatic cancer patient-derived organoids were either collected by surgical resection (B25) or endoscopic fine needle aspiration (B34) at Klinikum rechts der Isar der TU München, Germany. Patients were enrolled and consented according to the institutional review board (IRB) project-number 207/15 of the Technical University Munich. PDOs were characterized using whole exome sequencing and RNAseq as described previously (*43*). Human normal and adenocarcinoma pancreatic samples (>30% tumoral cells) were selected at IUCT-O clinic, and collected according French and European legislation (CRB Biobank, France with following ethical authorization numbers BB-0033-00014, DC-2008-463, AC-2013-1955). KPC and KPC; p110γ-/- mice were obtained and their genotype verified as described in (*27*).

In vitro culture of pancreatic cell lines and cell assays

Human pancreatic cancer cell lines Capan-1 and BxPC-3 were cultured in RMPI 1640 medium. PANC-1, MIA PaCa-2 and all murine pancreatic cancer cells were cultured in Dulbecco's Modified Eagle's Medium with 4.5g of glucose (D6429, Sigma). All media were supplemented with 10% fetal bovine serum (Eurobio), 1% glutamine (G7513, Sigma) and 1% antibiotics (penicillin/streptomycin, P0781, Sigma). Patient's organoids cell lines were cultured in special medium (Reichert composition,(*43*)). Specific methods to analyze cell proliferation/survival, mRNA and protein expression levels are described in **Supplementary Material &Methods**.

SILAC phosphoproteome and Bioinformatics analysis

Light amino acid-labelled and heavy amino acid-labelled Capan-1 cells (respectively called thereafter "light" and "heavy" cells) as described in **Supplementary Material &Methods** were washed twice with phosphate buffer saline (PBS; SIGMA; D8537), trypzined (GE Healthcare; L11-002) and plated at a concentration of $2.5.10^6$ cells in a 14.4cm-diameter dish (Dutscher, 055063). After 48h, cells were serum-starved during 16h, over-night. Light and heavy cells were pre-treated respectively with inhibitors or their accordingly diluted vehicule (DMSO)

during 1h, then stimulated or not for 10min or 24h with 2% dialyzed FBS. After 10min and 24h of FBS stimulation, heavy cells and light cells were maintained on ice, washed three times with cold PBS and lysed. Four biological replicates were sampled for each time point. These biological replicates were performed on four weeks. For each biological replicate, light lysates were mixed with the same heavy lysates at a 1:1 ratio for a total amount of 6 mg (**Figure 1C**). Protein samples were reduced with 100 mM DTT (Sigma, D9163) for 35 min at 57°C and then handled according to the FASP (Filter Aided Sample Preparation) digestion protocol (*44*) using Amicon Ultra-15 Centrifugal Filter device (10kDa cut-off, MILLIPORE, UFC901096). Protocol for the enrichment with TiO_2 beads is based on Larsen et al., (*45*) and Jensen et al. (*45*). SILAC samples (TiO_2 enriched peptides) were resuspended with 2% acetonitrile, 0.05% TFA and analyzed by nano-LC-MS/MS using an UltiMate 3000 system (Dionex) coupled to LTQ-Orbitrap Velos mass spectrometers (Thermo Fisher Scientific, Bremen, Germany). All 40 mass spectrometry proteomic files have been deposited to ProteomeXchange Consortium with the dataset identifier as listed in **Supplementary Table 1**. For peptide identification, raw data files were processed in Proteome Discover 1.4.1.14 (Thermo Scientific) and searched against SwissProt human fasta database of Mascot (2014-06, sprot_20140428.fasta, 542782 sequences, high and medium confidence, Q-value = 0.5-0.1). Peptides were further filtered using Mascot significance threshold S/N = 1.5 and a FDR <0.01 based on q-Value (Percolator). Phospho-site localization probabilities were calculated with *phospho*RS 3.1 (maximum PTMs per peptide 10, maximum position isoforms 200). Phosphopeptides filtered with Proteome Discoverer 1.4.1.14 (see criteria in **Supplementary Material &Methods**) were isolated from peptides. Only the ratios which were changed above and below the thresholds were processed for further analysis as described in **Supplementary Material &Methods**.

Statistics

Correlation between proliferation/survival effect and phospho-protein/protein expression levels were obtained by a principal component analysis (PCA) and the calculation of a Pearson r correlation factor, respectively with XLSTAT (version 2017.4, Addinsoft, USA) and GraphPad.

Heatmaps were performed using Genesis software (complete linkage hierarchical clustering). The median dose effect or half the maximal inhibitory concentration (IC50) values for each cell line at different time points were determined using CompuSyn software based on the quantitative analysis of dose–effect relationships on multiple drugs or enzyme inhibitors by Chou and Talalay (*46*). Combinational index (CI) values were calculated to confirm synergy. CI <1 indicates synergistic effects, CI = 1 indicates the mean additive effect of the drugs, and CI > 1 represents an antagonistic effect. Experimental data provided at least three biological replicates. Statistically significant differences were performed with GraphPad Prism using the T-tests (paired test): * $P < 0.05$, ** $P < 0.01$, *** $P < 0.001$. Non-significant (ns) if $P > 0.05$.

Acknowledgments We thank members of SigDYN group for constructive discussions, as well as members of CRCT core platforms, vectorology, cytometry and imaging, B Couderc for p110s-shRNA plasmids. **Funding** SigDYN group is a member of Labex TouCAN, ANR programme d'excellence on resistance to therapies in cancer. Laboratory of JGG for this project was funded by RITC, Université de Toulouse (Emergeance), Ligue Nationale Contre le Cancer (salary to CC and CC), Fondation pour la recherche Médicale FRM (salary to DT), Fondation FONROGA (CC), Fondation de France (salary to BT), MSCA-ITN-PhD (salary to RDF), COST PanGenEU and Université Paul Sabatier for French-German student exchange (to CC). MR was supported by the German Cancer Aid Foundation (Max Eder Program, Deutsche Krebshilfe 111273, MR) and the German Research Foundation (Deutsche Forschungsgemeinschaft, SFB1321 Modeling and Targeting Pancreatic Cancer). Laboratory of BSO was supported in part by the Région Midi-Pyrénées, European funds (Fonds Europeéns de Développement Régional, FEDER), Toulouse Métropole, and by the French Ministry of Research with the Investissement d'Avenir Infrastructures Nationales en Biologie et Santé program (ProFI, Proteomics French Infrastructure project, ANR-10-INBS-08). JGG and MR were awarded a Forcheur Jean-Marie Lehn Award on this project. **Author contributions** CC, DT, DZ, TN, CC, RDF, TB, CP: experiments; CC, DT, MBE, BMP, JGG: formal analysis of data; CC, DT, MBE, BMP, PF, GSB, BSO, MR, JGG: methodology; CC,

JGG: visualization of data; CC, TD, BMP: material and methods writing; CC, JGG: review of writing; all authors: editing MS; PC, HE, BGA, MR: provided samples; BSO, MR, JGG: supervision; JGG: conceptualization, funding acquisition, project administration, project supervision, validation, writing – original draft. **Competing interests:** WO2019101871-A1 & WO2019073031-A1 are filed patents pertaining to the results presented in the paper. **Data and materials availability:** Phosphoproteomics data has been deposited in Pride / ProteomeXchange with the dataset identifier PDX008410 the 11/12/2017. PDO, plasmids for sh expression used in the manuscript require an MTA.

Figure legends

Figure 1: Level of PI3K/Akt pathway activation in pancreatic cancer and strategy for the identification of core redundant PI3K-regulated signaling networks versus isoform-selective signaling networks. (A) Frozen samples of normal adjacent pancreas (NA, n=11 patients) and pancreatic cancer (PDAC, n=13 patients) samples were lysed. Phospho-effector abundance of PI3K/Akt/mTOR pathway was assessed by western blot using indicated antibodies, in samples comprising >30% of epithelial cells; quantification was performed only when the normal adjacent tissue was available (n=11 patients). Hierarchical clustering is shown using log (fold-change PDAC vs. normal adjacent). (B) Capan-1 pancreatic cancer cells were pre-treated with pan-PI3K, isoform-selective inhibitors (same conditions) or their accordingly diluted vehicle (DMSO) during 1h, then stimulated or not for 10min with 2% FBS. After 10min cells were lysed and phospho-effector abundance of PI3K/Akt/mTOR pathway was assessed by western blot using indicated antibodies and quantified (n≥4 independent biological replicates). Total Akt and Actin is used as a loading control. (C, D) Scheme of SILAC strategy to identify common or pan-PI3K and isoform-selective phosphorylation-regulated signaling pathways. Light amino acid-labelled and heavy amino acid-labelled Capan-1 cells were pre-treated respectively with 10µM LY-294002 (pan-inh), 5µM A66 (PI3Kα inhibitor

named α-inh), 500nM TGX-221 (PI3Kβ inhibitor named β-inh), 5µM AS-252424 (PI3Kγ inhibitor named γ-inh) or their accordingly diluted vehicle (DMSO) during 1h, then stimulated or not for 10min or 24h with 2% dialysed FBS. After 10min and 24h of FBS stimulation, heavy cells and light cells were lysed. For each biological replicate, light and heavy lysates were mixed at a 1:1 ratio, subjected to tryptic digestion and enrichment or not in phosphopeptides with TiO2 beads. Peptides were processed by mass spectrometry (Velos LTQ Orbitrap). Four biological replicates were sampled for each time point; light condition varies in the biological replicate while heavy vehicle condition is a technical replicate that is added in each run. Significantly increased/decreased phospho-peptides ratios (fold change = 2) for each condition are represented in D.

Figure 2: Class I PI3K isoforms regulate distinct signaling pathways in pancreatic cancer cells. (A) Global variation of phosphoproteome under FBS stimulation with or without PI3K inhibitor treatment in Capan-1 at 10min and 24h. Principal component analysis (PCA) analysis is shown. n=4 independent biological replicates. (B) Representation of targets specifically modified by pan-PI3K, PI3Kα, PI3Kβ and PI3Kγ inhibition. Dashed lines explain how core phosphopeptides are defined. A Venn diagram of modified phosphopeptides in at least one condition at each time point is shown. n=4 independent biological replicates. (C) Enrichments of biological pathways found in the list of core, pan-, isoform-selective phosphoproteins at 10min and 24h were performed with AutoCompare software (pvalue ≤ 0.01). n=4 independent biological replicates.

Figure 3: PI3Kγ is overexpressed albeit at low levels in pancreatic cancer tumor cells. (A) Frozen samples of normal adjacent pancreas (NA, n=11 patients) and pancreatic cancer (PDAC, n=13 patients) samples were lysed. PI3K isoforms proteins pattern of expression was assessed by western blot using indicated antibodies, in samples comprising >30% of epithelial cells, and quantified when the adjacent tissue was available. Hierarchical clustering is shown using log (fold-change PDAC vs. normal adjacent). (B-C) Human and murine pancreatic cells

were lysed. PI3K isoform mRNA and protein pattern of expression was evaluated by RT-qPCR and WB. Mean ± SEM is shown, WB: n=3 human n=1 murine, qPCR: n=3 human, n=2 murine, independent biological replicates.

Figure 4: PI3Kγ-selective inhibitor sensitivity on the survival of pancreatic cancer cells. (A) Incidence of cancer in KPC (n=8 mice) versus KPC;p110γ-/- mice (n=7 mice). Representative pictures are shown. Scale=50µm (B) Validation of efficient down-regulation protein expression of p110γ targeting by genetic inhibition (shRNA) of Capan-1 cells. Number of colonies in soft agar assay of established cell lines (n=4 independent biological replicates; mean of 4 replicates ± SEM is shown). (C,D) Human pancreatic cancer cells activation of PI3K and survival were evaluated by western blot(10min) and MTT after 24h, 48h, 72h, day 6 with or without PI3K inhibitors or vehicle without 2% of FBS (n≥3 independent biological replicates; OD mean ± SEM is shown).

Figure 5: Combination of PI3Kγ and PI3Kα inhibitors lead to synergistic effect on cell survival in pancreatic ductal adenocarcinoma patients. (A) 24h of PI3K/Akt/mTOR signalling pathway activation with 2% FBS (n>3) and pan-PI3K inhibitor (n>3), PI3Kγ-inhibitor (n>3), PI3Kα-inhibitor (n>3) or dual inhibition PI3Kγ/PI3Kα (n=2) by western blot using indicated antibodies in Capan-1, BxPC-3, Panc-1 and MIA PaCa-2 cells. (B) Genetic landscape of PDAC organoids (n=2 patients). MAF=Minor Allele Frequency. (C) Level of expression of PI3K-related genes (Illumina) (n=2 patients). (D) Sensitivity to PI3K inhibition, as indicated, on morphological and number of two human pancreatic cancer primary cultures cultured in organoid condition, named B25 and B34, after 5 days of treatment. Representative pictures are shown. Scale bars=50µm (n=3 independent biological replicates). Black triangle= normal organoids; orange triangle=severely altered organoids. (E) Dose-response of two human pancreatic primary organoids viability were evaluated by CellGlo Titer assay after 5 days in complete medium with or without PI3K inhibitors, as indicated (n=3 independent biological replicates; mean ± SEM is shown). (F) Evaluation of synergistic action on survival of

7 human pancreatic cancer cells cultured in 2D (Capan-1, BxPC-3, Panc-1 and MIA PaCa-2) and 3D (B25 and B34) was performed determined using CompuSyn software based on the quantitative analysis of dose–effect relationships on multiple drugs. Combinational index (CI) values were calculated to evaluate synergy. CI < 1 indicates synergistic effects, 0.8 ≥ CI ≤ 1.2 indicates an additive effect, and CI > 1 represents an antagonistic effect (n≥3 independent biological replicates; mean ± SEM was used).

References

1. B. Vanhaesebroeck, J. Guillermet-Guibert, M. Graupera, B. Bilanges, The emerging mechanisms of isoform-specific PI3K signalling. *Nat. Rev. Mol. Cell Biol.* **11**, 329–341 (2010).

2. M. S. Lawrence, P. Stojanov, C. H. Mermel, J. T. Robinson, L. A. Garraway, T. R. Golub, M. Meyerson, S. B. Gabriel, E. S. Lander, G. Getz, Discovery and saturation analysis of cancer genes across 21 tumour types. *Nature*. **505**, 495–501 (2014).

3. E. Pons-Tostivint, B. Thibault, J. Guillermet-Guibert, Targeting PI3K Signaling in Combination Cancer Therapy. *Trends Cancer*. **3**, 454–469 (2017).

4. H. Al-Qassab, M. A. Smith, E. E. Irvine, J. Guillermet-Guibert, M. Claret, A. I. Choudhury, C. Selman, K. Piipari, M. Clements, S. Lingard, K. Chandarana, J. D. Bell, G. S. Barsh, A. J. H. Smith, R. L. Batterham, M. L. J. Ashford, B. Vanhaesebroeck, D. J. Withers, Dominant role of the p110beta isoform of PI3K over p110alpha in energy homeostasis regulation by POMC and AgRP neurons. *Cell Metab.* **10**, 343–354 (2009).

5. V. Martin, J. Guillermet-Guibert, G. Chicanne, C. Cabou, M. Jandrot-Perrus, M. Plantavid, B. Vanhaesebroeck, B. Payrastre, M.-P. Gratacap, Deletion of the p110beta isoform of phosphoinositide 3-kinase in platelets reveals its central role in Akt activation and thrombus formation in vitro and in vivo. *Blood*. **115**, 2008–2013 (2010).

6. M. Graupera, J. Guillermet-Guibert, L. C. Foukas, L.-K. Phng, R. J. Cain, A. Salpekar, W. Pearce, S. Meek, J. Millan, P. R. Cutillas, A. J. H. Smith, A. J. Ridley, C. Ruhrberg, H. Gerhardt, B. Vanhaesebroeck, Angiogenesis selectively requires the p110alpha isoform of PI3K to control endothelial cell migration. *Nature*. **453**, 662–666 (2008).

7. J. Guillermet-Guibert, K. Bjorklof, A. Salpekar, C. Gonella, F. Ramadani, A. Bilancio, S. Meek, A. J. H. Smith, K. Okkenhaug, B. Vanhaesebroeck, The p110beta isoform of phosphoinositide 3-kinase signals downstream of G protein-coupled receptors and is functionally redundant with p110gamma. *Proc. Natl. Acad. Sci. U.S.A.* **105**, 8292–8297 (2008).

8. F. André, E. Ciruelos, G. Rubovszky, M. Campone, S. Loibl, H. S. Rugo, H. Iwata, P. Conte, I. A. Mayer, B. Kaufman, T. Yamashita, Y.-S. Lu, K. Inoue, M. Takahashi, Z. Pápai, A.-S. Longin, D. Mills, C. Wilke, S. Hirawat, D. Juric, Alpelisib for *PIK3CA* -Mutated, Hormone Receptor–Positive Advanced Breast Cancer. *New England Journal of Medicine*. **380**, 1929–1940 (2019).

9. K. M. Vasudevan, D. A. Barbie, M. A. Davies, R. Rabinovsky, C. J. McNear, J. J. Kim, B. T. Hennessy, H. Tseng, P. Pochanard, S. Y. Kim, I. F. Dunn, A. C. Schinzel, P. Sandy, S. Hoersch, Q. Sheng, P. B. Gupta, J. S. Boehm, J. H. Reiling, S. Silver, Y. Lu, K. Stemke-Hale, B. Dutta, C. Joy, A. A. Sahin, A. M. Gonzalez-Angulo, A. Lluch, L. E. Rameh, T. Jacks, D. E. Root, E. S. Lander, G. B. Mills, W. C. Hahn, W. R. Sellers, L. A. Garraway, AKT-independent signaling downstream of oncogenic PIK3CA mutations in human cancer. *Cancer Cell*. **16**, 21–32 (2009).

10. E. Castellano, J. Downward, RAS Interaction with PI3K: More Than Just Another Effector Pathway. *Genes Cancer*. **2**, 261–274 (2011).

11. C. Costa, H. Ebi, M. Martini, S. A. Beausoleil, A. C. Faber, C. T. Jakubik, A. Huang, Y. Wang, M. Nishtala, B. Hall, K. Rikova, J. Zhao, E. Hirsch, C. H. Benes, J. A. Engelman, Measurement of PIP3 levels reveals an unexpected role for p110β in early adaptive responses to p110α-specific inhibitors in luminal breast cancer. *Cancer Cell*. **27**, 97–108 (2015).

12. S. Schwartz, J. Wongvipat, C. B. Trigwell, U. Hancox, B. S. Carver, V. Rodrik-Outmezguine, M. Will, P. Yellen, E. de Stanchina, J. Baselga, H. I. Scher, S. T. Barry, C. L. Sawyers, S. Chandarlapaty, N. Rosen, Feedback suppression of PI3Kα signaling in PTEN-mutated tumors is relieved by selective inhibition of PI3Kβ. *Cancer Cell*. **27**, 109–122 (2015).

13. D. Zecchin, C. Moore, F. Michailidis, S. Horswell, S. Rana, M. Howell, J. Downward, Combined targeting of G protein-coupled receptor and EGF receptor signaling overcomes resistance to PI 3K pathway inhibitors in PTEN -null triple negative breast cancer. *EMBO Mol Med*. **12** (2020), doi:10.15252/emmm.202011987.

14. M. G. Schlieman, B. N. Fahy, R. Ramsamooj, L. Beckett, R. J. Bold, Incidence, mechanism and prognostic value of activated AKT in pancreas cancer. *Br. J. Cancer*. **89**, 2110–2115 (2003).

15. B. Kong, W. Wu, T. Cheng, A. M. Schlitter, C. Qian, P. Bruns, Z. Jian, C. Jäger, I. Regel, S. Raulefs, N. Behler, M. Irmler, J. Beckers, H. Friess, M. Erkan, J. T. Siveke, A. Tannapfel, S. A. Hahn, F. J. Theis, I. Esposito, J. Kleeff, C. W. Michalski, A subset of metastatic pancreatic ductal adenocarcinomas depends quantitatively on oncogenic Kras/Mek/Erk-induced hyperactive mTOR signalling. *Gut*. **65**, 647–657 (2016).

16. R. Baer, C. Cintas, M. Dufresne, S. Cassant-Sourdy, N. Schönhuber, L. Planque, H. Lulka, B. Couderc, C. Bousquet, B. Garmy-Susini, B. Vanhaesebroeck, S. Pyronnet, D. Saur, J. Guillermet-Guibert, Pancreatic cell plasticity and cancer initiation induced by oncogenic Kras is completely dependent on wild-type PI 3-kinase p110α. *Genes Dev.* **28**, 2621–2635 (2014).

17. C.-Y. C. Wu, E. S. Carpenter, K. K. Takeuchi, C. J. Halbrook, L. V. Peverley, H. Bien, J. C. Hall, K. E. DelGiorno, D. Pal, Y. Song, C. Shi, R. Z. Lin, H. C. Crawford, PI3K regulation of RAC1 is required for KRAS-induced pancreatic tumorigenesis in mice. *Gastroenterology*. **147**, 1405-1416.e7 (2014).

18. G. A. Hobbs, N. M. Baker, A. M. Miermont, R. D. Thurman, M. Pierobon, T. H. Tran, A. O. Anderson, A. M. Waters, J. N. Diehl, B. Papke, R. G. Hodge, J. E. Klomp, C. M. Goodwin, J. M. DeLiberty, J. Wang, R. W. S. Ng, P. Gautam, K. L. Bryant, D. Esposito, S. L. Campbell, E. F. Petricoin, D. K. Simanshu, A. J. Aguirre, B. M. Wolpin, K. Wennerberg, U. Rudloff, A. D. Cox, C. J. Der, Atypical KRASG12R Mutant Is Impaired in

PI3K Signaling and Macropinocytosis in Pancreatic Cancer. *Cancer Discov*. **10**, 104–123 (2020).

19. C. Cayron, J. Guillermet-Guibert, The type of KRAS mutation drives PI3Kα/γ signalling dependency: Implication for the choice of targeted therapy in pancreatic adenocarcinoma patients. *Clin Res Hepatol Gastroenterol* (2020), doi:10.1016/j.clinre.2020.05.021.

20. S. Gupta, A. R. Ramjaun, P. Haiko, Y. Wang, P. H. Warne, B. Nicke, E. Nye, G. Stamp, K. Alitalo, J. Downward, Binding of Ras to Phosphoinositide 3-Kinase p110α Is Required for Ras- Driven Tumorigenesis in Mice. *Cell*. **129**, 957–968 (2007).

21. S. Mueller, T. Engleitner, R. Maresch, M. Zukowska, S. Lange, T. Kaltenbacher, B. Konukiewitz, R. Öllinger, M. Zwiebel, A. Strong, H.-Y. Yen, R. Banerjee, S. Louzada, B. Fu, B. Seidler, J. Götzfried, K. Schuck, Z. Hassan, A. Arbeiter, N. Schönhuber, S. Klein, C. Veltkamp, M. Friedrich, L. Rad, M. Barenboim, C. Ziegenhain, J. Hess, O. M. Dovey, S. Eser, S. Parekh, F. Constantino-Casas, J. de la Rosa, M. I. Sierra, M. Fraga, J. Mayerle, G. Klöppel, J. Cadiñanos, P. Liu, G. Vassiliou, W. Weichert, K. Steiger, W. Enard, R. M. Schmid, F. Yang, K. Unger, G. Schneider, I. Varela, A. Bradley, D. Saur, R. Rad, Evolutionary routes and KRAS dosage define pancreatic cancer phenotypes. *Nature*. **554**, 62–68 (2018).

22. C. Cintas, T. Douche, N. Therville, S. Arcucci, F. Ramos-Delgado, C. Basset, B. Thibault, J. Guillermet-Guibert, Signal-Targeted Therapies and Resistance Mechanisms in Pancreatic Cancer: Future Developments Reside in Proteomics. *Cancers*. **10** (2018), doi:10.3390/cancers10060174.

23. J. R. Conway, D. Herrmann, T. J. Evans, J. P. Morton, P. Timpson, Combating pancreatic cancer with PI3K pathway inhibitors in the era of personalised medicine. *Gut*. **68**, 742–758 (2019).

24. Cancer Genome Atlas Research Network. Electronic address: andrew_aguirre@dfci.harvard.edu, Cancer Genome Atlas Research Network, Integrated Genomic Characterization of Pancreatic Ductal Adenocarcinoma. *Cancer Cell*. **32**, 185-203.e13 (2017).

25. R. Baer, C. Cintas, N. Therville, J. Guillermet-Guibert, Implication of PI3K/Akt pathway in pancreatic cancer: When PI3K isoforms matter? *Adv Biol Regul*. **59**, 19–35 (2015).

26. C. E. Edling, F. Selvaggi, R. Buus, T. Maffucci, P. Di Sebastiano, H. Friess, P. Innocenti, H. M. Kocher, M. Falasca, Key role of phosphoinositide 3-kinase class IB in pancreatic cancer. *Clin. Cancer Res.* **16**, 4928–4937 (2010).

27. M. M. Kaneda, P. Cappello, A. V. Nguyen, N. Ralainirina, C. R. Hardamon, P. Foubert, M. C. Schmid, P. Sun, E. Mose, M. Bouvet, A. M. Lowy, M. A. Valasek, R. Sasik, F. Novelli, E. Hirsch, J. A. Varner, Macrophage PI3Kγ Drives Pancreatic Ductal Adenocarcinoma Progression. *Cancer Discov*. **6**, 870–885 (2016).

28. C. Basset, J. Guillermet-Guibert, Attenuating PI3K isoforms in pancreatic cancer: Focus on immune PI3Kgamma. *Clinics and research in hepatology and gastroenterology*. **41**, 351–353 (2017).

29. S. Jamieson, J. U. Flanagan, S. Kolekar, C. Buchanan, J. D. Kendall, W.-J. Lee, G. W. Rewcastle, W. A. Denny, R. Singh, J. Dickson, B. C. Baguley, P. R. Shepherd, A drug targeting only p110α can block phosphoinositide 3-kinase signalling and tumour growth in certain cell types. *Biochem. J.* **438**, 53–62 (2011).

30. J. Guillermet-Guibert, L. B. Smith, G. Halet, M. A. Whitehead, W. Pearce, D. Rebourcet, K. León, P. Crépieux, G. Nock, M. Strömstedt, M. Enerback, C. Chelala, M. Graupera, J. Carroll, S. Cosulich, P. T. K. Saunders, I. Huhtaniemi, B. Vanhaesebroeck, Novel Role for p110β PI 3-Kinase in Male Fertility through Regulation of Androgen Receptor Activity in Sertoli Cells. *PLoS Genet.* **11**, e1005304 (2015).

31. V. Pomel, J. Klicic, D. Covini, D. D. Church, J. P. Shaw, K. Roulin, F. Burgat-Charvillon, D. Valognes, M. Camps, C. Chabert, C. Gillieron, B. Françon, D. Perrin, D. Leroy, D. Gretener, A. Nichols, P. A. Vitte, S. Carboni, C. Rommel, M. K. Schwarz, T. Rückle, Furan-2-ylmethylene thiazolidinediones as novel, potent, and selective inhibitors of phosphoinositide 3-kinase gamma. *J. Med. Chem.* **49**, 3857–3871 (2006).

32. T. Geiger, J. R. Wisniewski, J. Cox, S. Zanivan, M. Kruger, Y. Ishihama, M. Mann, Use of stable isotope labeling by amino acids in cell culture as a spike-in standard in quantitative proteomics. *Nat Protoc*. **6**, 147–157 (2011).

33. A. Shenoy, T. Geiger, Super-SILAC: current trends and future perspectives. *Expert Review of Proteomics*. **12**, 13–19 (2015).

34. S. S. Ng, M. S. Tsao, T. Nicklee, D. W. Hedley, Wortmannin inhibits pkb/akt phosphorylation and promotes gemcitabine antitumor activity in orthotopic human pancreatic cancer xenografts in immunodeficient mice. *Clin. Cancer Res.* **7**, 3269–3275 (2001).

35. S. Diersch, P. Wenzel, M. Szameitat, P. Eser, M. C. Paul, B. Seidler, S. Eser, M. Messer, M. Reichert, P. Pagel, I. Esposito, R. M. Schmid, D. Saur, G. Schneider, Efemp1 and p27(Kip1) modulate responsiveness of pancreatic cancer cells towards a dual PI3K/mTOR inhibitor in preclinical models. *Oncotarget*. **4**, 277–288 (2013).

36. H. P. Soares, M. Ming, M. Mellon, S. H. Young, L. Han, J. Sinnet-Smith, E. Rozengurt, Dual PI3K/mTOR Inhibitors Induce Rapid Overactivation of the MEK/ERK Pathway in Human Pancreatic Cancer Cells through Suppression of mTORC2. *Mol. Cancer Ther.* **14**, 1014–1023 (2015).

37. H. Zhong, C. Sanchez, D. Spitzer, D. Spitrzer, S. Plambeck-Suess, J. Gibbs, W. G. Hawkins, D. Denardo, F. Gao, R. A. Pufahl, A. C. Lockhart, M. Xu, D. Linehan, J. Weber, A. Wang-Gillam, Synergistic effects of concurrent blockade of PI3K and MEK pathways in pancreatic cancer preclinical models. *PLoS ONE*. **8**, e77243 (2013).

38. B. Alagesan, G. Contino, A. R. Guimaraes, R. B. Corcoran, V. Deshpande, G. R. Wojtkiewicz, A. F. Hezel, K.-K. Wong, M. Loda, R. Weissleder, C. H. Benes, J. Engelman, N. Bardeesy, Combined MEK and PI3K inhibition in a mouse model of pancreatic cancer. *Clin. Cancer Res.* **21**, 396–404 (2015).

39. L. C. Foukas, I. M. Berenjeno, A. Gray, A. Khwaja, B. Vanhaesebroeck, Activity of any class IA PI3K isoform can sustain cell proliferation and survival. *Proc. Natl. Acad. Sci. U.S.A.* **107**, 11381–11386 (2010).

40. D. Juric, P. Castel, M. Griffith, O. L. Griffith, H. H. Won, H. Ellis, S. H. Ebbesen, B. J. Ainscough, A. Ramu, G. Iyer, R. H. Shah, T. Huynh, M. Mino-Kenudson, D. Sgroi, S. Isakoff, A. Thabet, L. Elamine, D. B. Solit, S. W. Lowe, C. Quadt, M. Peters, A. Derti, R. Schegel, A. Huang, E. R. Mardis, M. F. Berger, J. Baselga, M. Scaltriti, Convergent loss of PTEN leads to clinical resistance to a PI(3)Kα inhibitor. *Nature*. **518**, 240–244 (2015).

41. C. Cintas, J. Guillermet-Guibert, Heterogeneity of Phosphatidylinositol-3-Kinase (PI3K)/AKT/Mammalian Target of Rapamycin Activation in Cancer: Is PI3K Isoform Specificity Important? *Front Oncol*. **7**, 330 (2017).

42. C. Torres, G. Mancinelli, J. Cordoba-Chacon, N. Viswakarma, K. Castellanos, S. Grimaldo, S. Kumar, D. Principe, M. J. Dorman, R. McKinney, E. Hirsch, D. Dawson, H. G. Munshi, A. Rana, P. J. Grippo, p110γ deficiency protects against pancreatic carcinogenesis yet predisposes to diet-induced hepatotoxicity. *Proc. Natl. Acad. Sci. U.S.A.* **116**, 14724–14733 (2019).

43. B. W. Renz, R. Takahashi, T. Tanaka, M. Macchini, Y. Hayakawa, Z. Dantes, H. C. Maurer, X. Chen, Z. Jiang, C. B. Westphalen, M. Ilmer, G. Valenti, S. K. Mohanta, A. J. R. Habenicht, M. Middelhoff, T. Chu, K. Nagar, Y. Tailor, R. Casadei, M. Di Marco, A. Kleespies, R. A. Friedman, H. Remotti, M. Reichert, D. L. Worthley, J. Neumann, J. Werner, A. C. Iuga, K. P. Olive, T. C. Wang, β2 Adrenergic-Neurotrophin Feedforward Loop Promotes Pancreatic Cancer. *Cancer Cell*. **33**, 75-90.e7 (2018).

44. J. R. Wiśniewski, A. Zougman, N. Nagaraj, M. Mann, Universal sample preparation method for proteome analysis. *Nature Methods*. **6**, 359–362 (2009).

45. M. R. Larsen, T. E. Thingholm, O. N. Jensen, P. Roepstorff, T. J. D. Jørgensen, Highly selective enrichment of phosphorylated peptides from peptide mixtures using titanium dioxide microcolumns. *Mol. Cell Proteomics*. **4**, 873–886 (2005).

46. T.-C. Chou, Drug combination studies and their synergy quantification using the Chou-Talalay method. *Cancer Res.* **70**, 440–446 (2010).

47. U. K. Aryal, A. R. S. Ross, Enrichment and analysis of phosphopeptides under different experimental conditions using titanium dioxide affinity chromatography and mass spectrometry. *Rapid Commun. Mass Spectrom.* **24**, 219–231 (2010).

48. B. Ycart, F. Pont, J.-J. Fournié, Curbing false discovery rates in interpretation of genome-wide expression profiles. *J Biomed Inform*. **47**, 58–61 (2014).

Figure 1

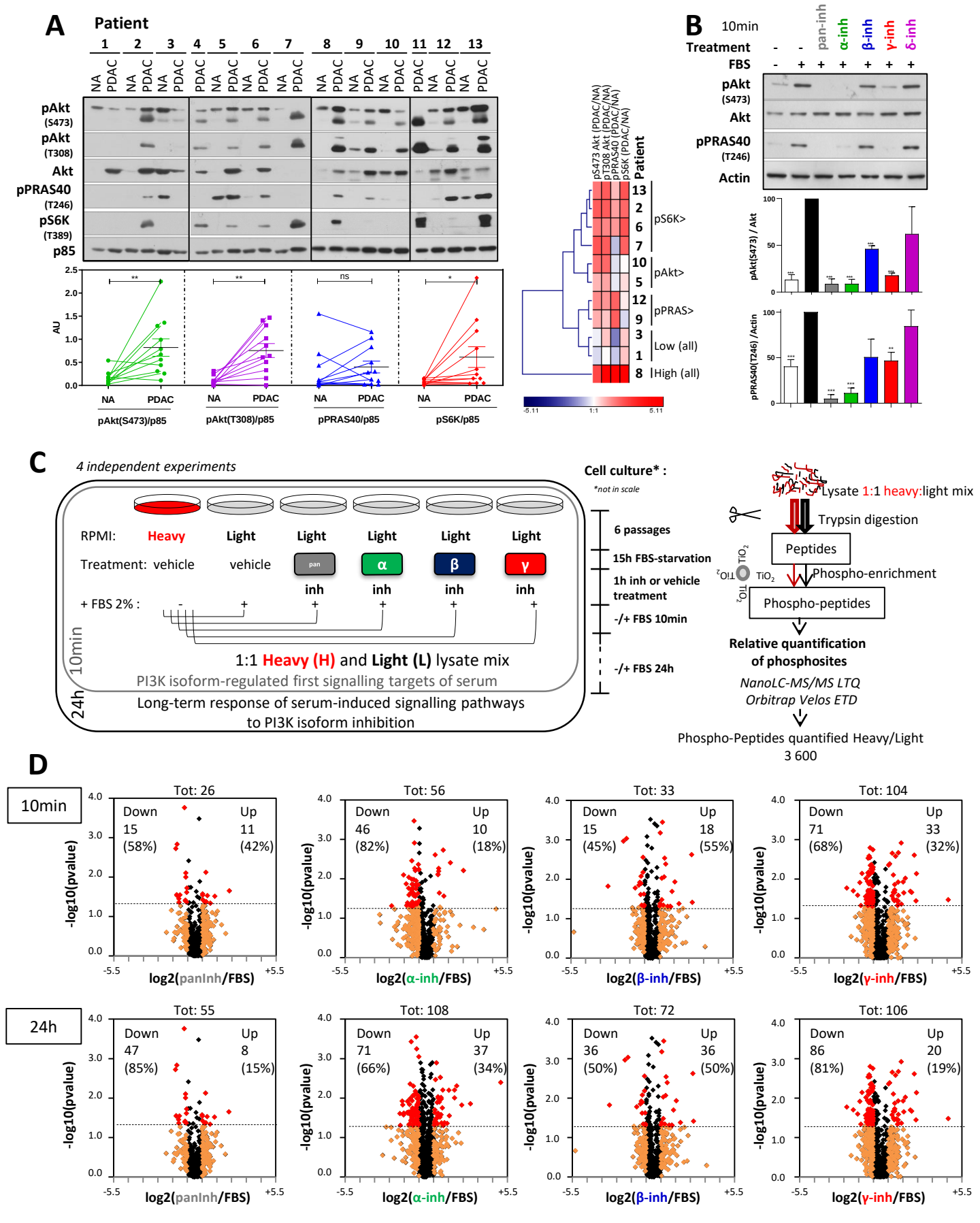
A
Patient
1 2 3 4 5 6 7 8 9 10 11 12 13
NA PDAC
pAkt (S473)
pAkt (T308)
Akt
pPRAS40 (T246)
pS6K (T389)
p85
AU
pAkt(S473)/p85
pAkt(T308)/p85
pPRAS40/p85
pS6K/p85
pS473 Akt (PDAC/NA)
pT308 Akt (PDAC/NA)
pPRAS40 (PDAC/NA)
pS6K (PDAC/NA)
Patient
pS6K>
pAkt>
pPRAS>
Low (all)
High (all)
B
10min
Treatment
FBS
pan-inh
α-inh
β-inh
γ-inh
δ-inh
pAkt (S473)
Akt
pPRAS40 (T246)
Actin
pAkt(S473) / Akt
pPRAS40(T246) /Actin
C
4 independent experiments
Cell culture* :
*not in scale
RPMI:
Heavy
Light
Treatment: vehicle
pan inh
α inh
β inh
γ inh
+ FBS 2% :
10min
1:1 Heavy (H) and Light (L) lysate mix
PI3K isoform-regulated first signalling targets of serum
24h
Long-term response of serum-induced signalling pathways to PI3K isoform inhibition
6 passages
15h FBS-starvation
1h inh or vehicle treatment
-/+ FBS 10min
-/+ FBS 24h
Lysate 1:1 heavy:light mix
Trypsin digestion
Peptides
Phospho-enrichment
Phospho-peptides
Relative quantification of phosphosites
NanoLC-MS/MS LTQ Orbitrap Velos ETD
Phospho-Peptides quantified Heavy/Light
3 600
D
10min
24h
Tot: 26
Down 15 (58%)
Up 11 (42%)
Tot: 56
Down 46 (82%)
Up 10 (18%)
Tot: 33
Down 15 (45%)
Up 18 (55%)
Tot: 104
Down 71 (68%)
Up 33 (32%)
Tot: 55
Down 47 (85%)
Up 8 (15%)
Tot: 108
Down 71 (66%)
Up 37 (34%)
Tot: 72
Down 36 (50%)
Up 36 (50%)
Tot: 106
Down 86 (81%)
Up 20 (19%)
-log10(pvalue)
log2(paninh/FBS)
log2(α-inh/FBS)
log2(β-inh/FBS)
log2(γ-inh/FBS)

Figure 2

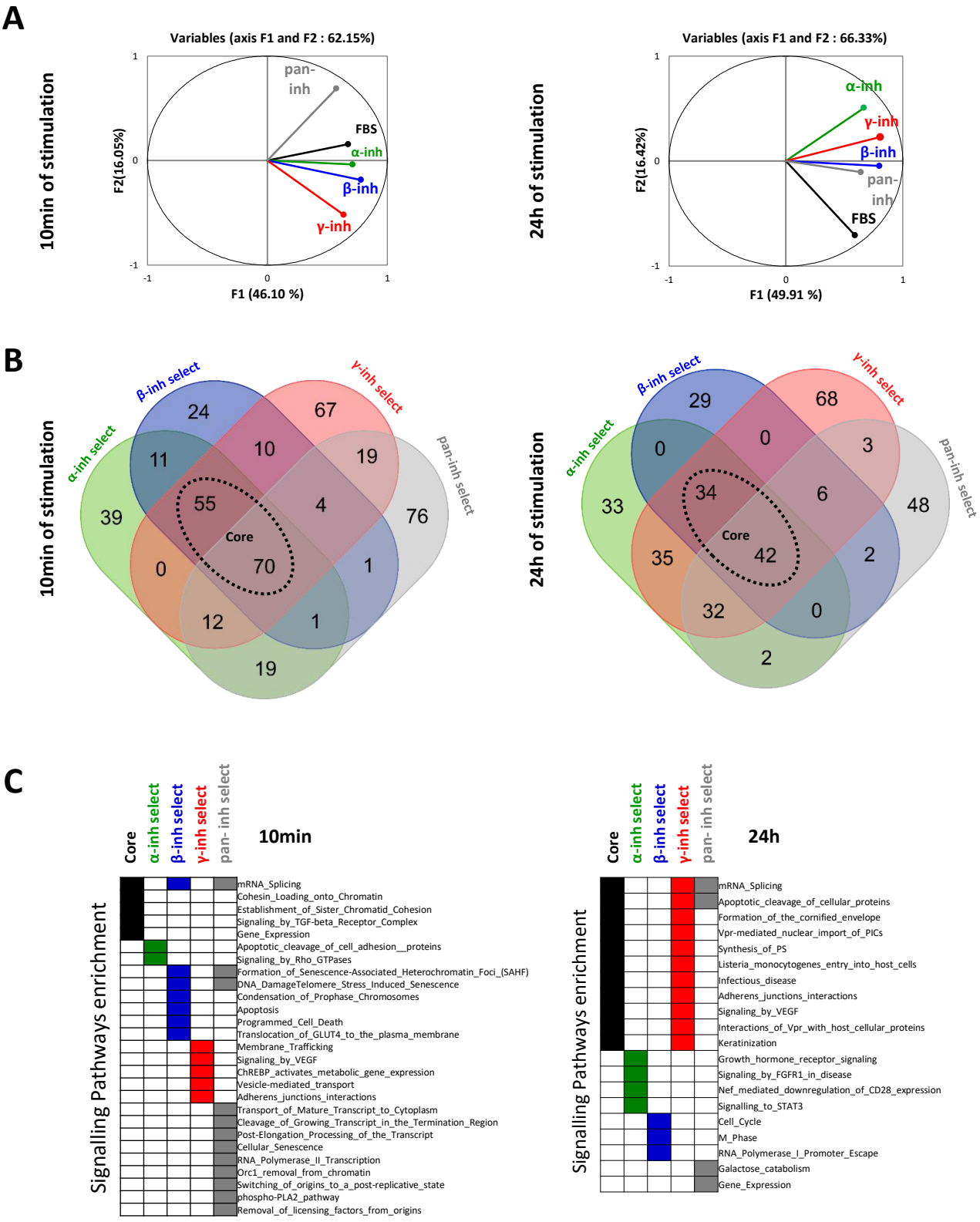
A
10min of stimulation
Variables (axis F1 and F2 : 62.15%)
F2(16.05%)
F1 (46.10 %)
pan-inh
FBS
α-inh
β-inh
γ-inh
24h of stimulation
Variables (axis F1 and F2 : 66.33%)
F2(16.42%)
F1 (49.91 %)
α-inh
γ-inh
β-inh
pan-inh
FBS
B
10min of stimulation
α-inh select
β-inh select
γ-inh select
pan-inh select
Core
24h of stimulation
C
Core
α-inh select
β-inh select
γ-inh select
pan- inh select
10min
Signalling Pathways enrichment
mRNA_Splicing
Cohesin_Loading_onto_Chromatin
Establishment_of_Sister_Chromatid_Cohesion
Signaling_by_TGF-beta_Receptor_Complex
Gene_Expression
Apoptotic_cleavage_of_cell_adhesion__proteins
Signaling_by_Rho_GTPases
Formation_of_Senescence-Associated_Heterochromatin_Foci_(SAHF)
DNA_DamageTelomere_Stress_Induced_Senescence
Condensation_of_Prophase_Chromosomes
Apoptosis
Programmed_Cell_Death
Translocation_of_GLUT4_to_the_plasma_membrane
Membrane_Trafficking
Signaling_by_VEGF
ChREBP_activates_metabolic_gene_expression
Vesicle-mediated_transport
Adherens_junctions_interactions
Transport_of_Mature_Transcript_to_Cytoplasm
Cleavage_of_Growing_Transcript_in_the_Termination_Region
Post-Elongation_Processing_of_the_Transcript
Cellular_Senescence
RNA_Polymerase_II_Transcription
Orc1_removal_from_chromatin
Switching_of_origins_to_a_post-replicative_state
phospho-PLA2_pathway
Removal_of_licensing_factors_from_origins
24h
Apoptotic_cleavage_of_cellular_proteins
Formation_of_the_cornified_envelope
Vpr-mediated_nuclear_import_of_PICs
Synthesis_of_PS
Listeria_monocytogenes_entry_into_host_cells
Infectious_disease
Adherens_junctions_interactions
Signaling_by_VEGF
Interactions_of_Vpr_with_host_cellular_proteins
Keratinization
Growth_hormone_receptor_signaling
Signaling_by_FGFR1_in_disease
Nef_mediated_downregulation_of_CD28_expression
Signalling_to_STAT3
Cell_Cycle
M_Phase
RNA_Polymerase_I_Promoter_Escape
Galactose_catabolism
Gene_Expression

Figure 3

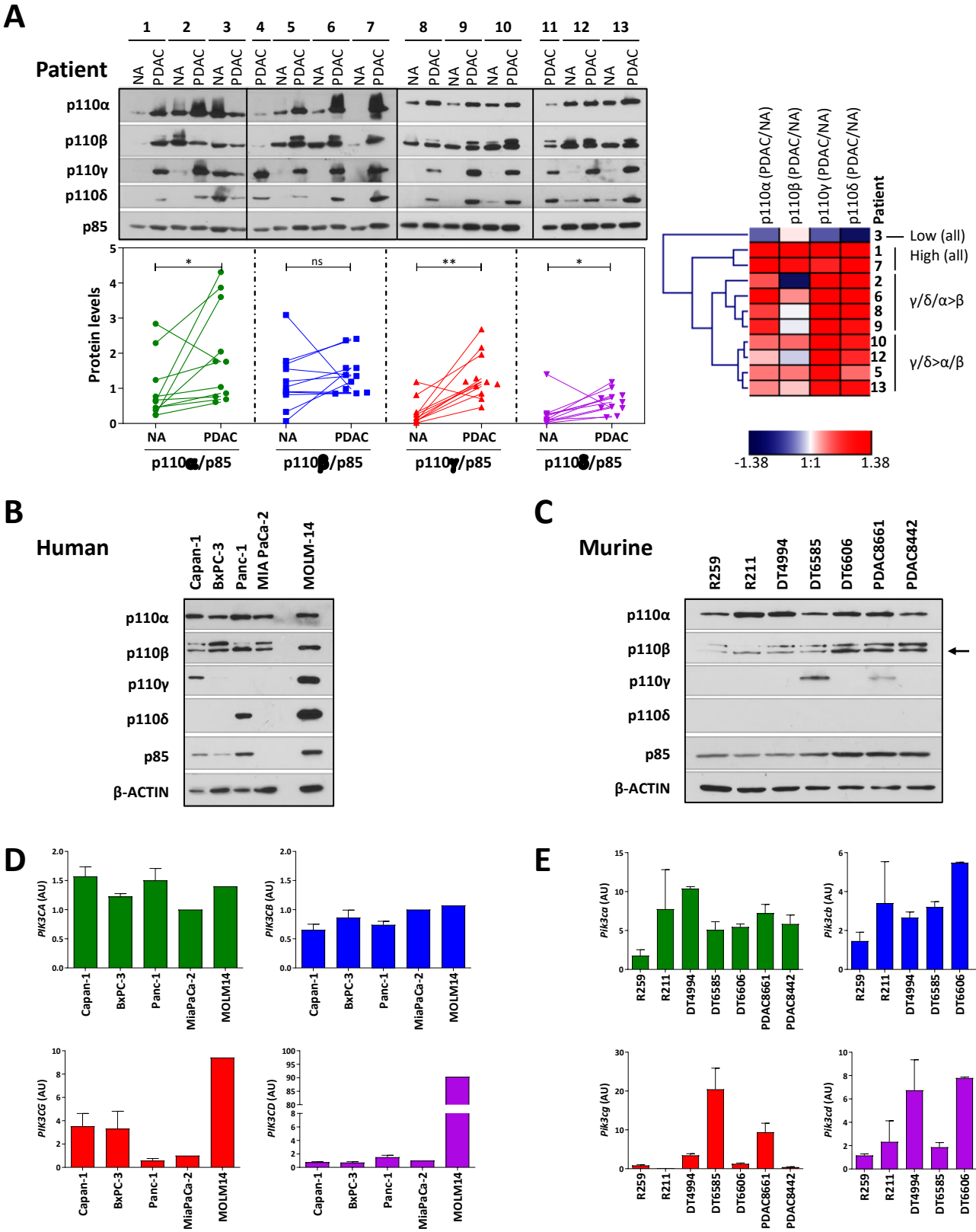
A
Patient
1 2 3 4 5 6 7 8 9 10 11 12 13
NA PDAC
p110α
p110β
p110γ
p110δ
p85
Protein levels
NA PDAC
p110α/p85
p110β/p85
p110γ/p85
p110δ/p85
p110α (PDAC/NA)
p110β (PDAC/NA)
p110γ (PDAC/NA)
p110δ (PDAC/NA)
Patient
Low (all)
High (all)
γ/δ/α>β
γ/δ>α/β
-1.38
1:1
1.38
B
Human
Capan-1
BxPC-3
Panc-1
MIA PaCa-2
MOLM-14
β-ACTIN
C
Murine
R259
R211
DT4994
DT6585
DT6606
PDAC8661
PDAC8442
D
PIK3CA (AU)
PIK3CB (AU)
PIK3CG (AU)
PIK3CD (AU)
Capan-1
BxPC-3
Panc-1
MiaPaCa-2
MOLM14
E
Pik3ca (AU)
Pik3cb (AU)
Pik3cg (AU)
Pik3cd (AU)

Figure 4

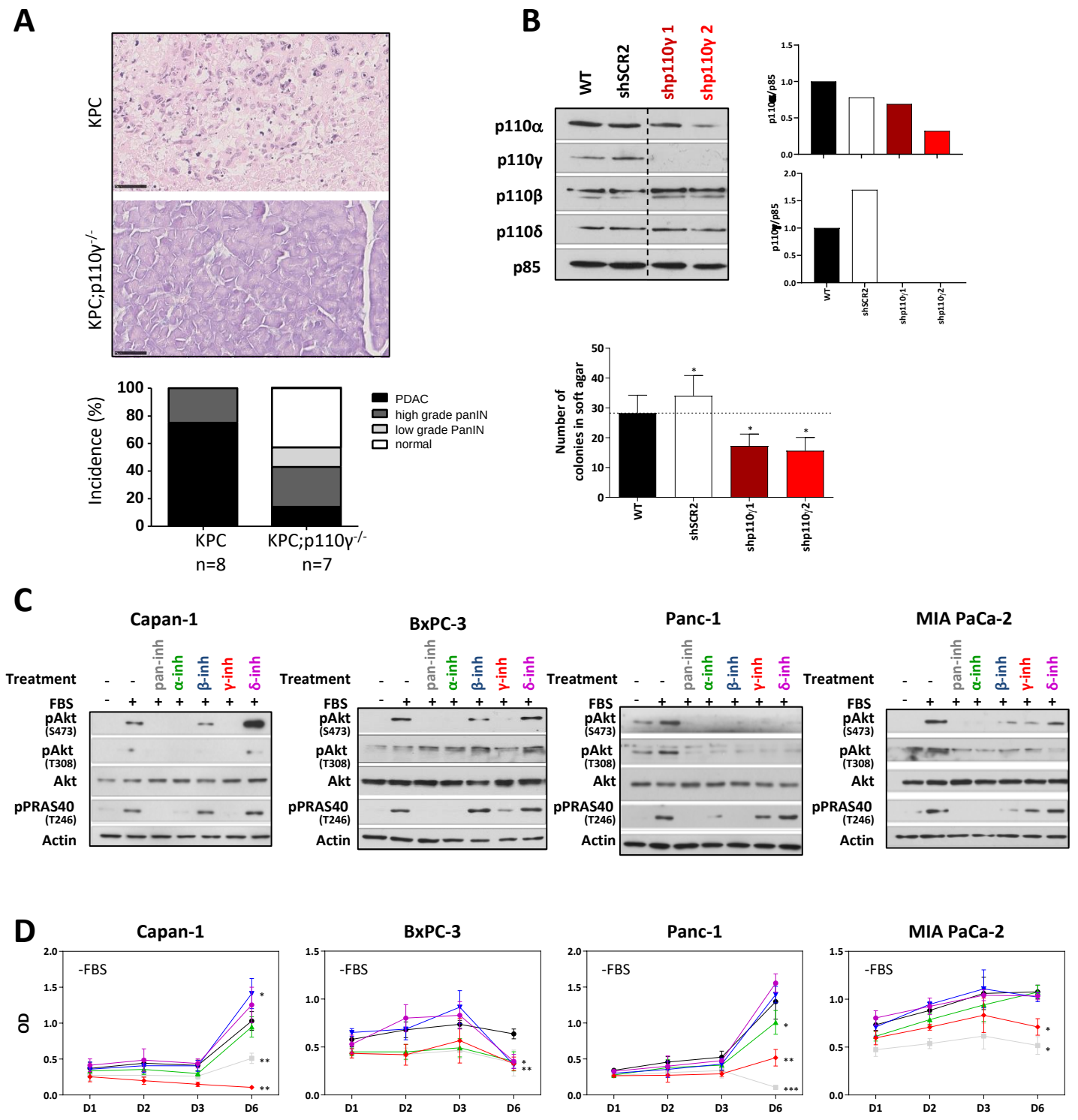
A
KPC
KPC;p110γ-/-
Incidence (%)
100
80
60
40
20
0
KPC
n=8
KPC;p110γ-/-
n=7
PDAC
high grade panIN
low grade PanIN
normal
B
WT
shSCR2
shp110γ 1
shp110γ 2
p110α
p110γ
p110β
p110δ
p85
p110α/p85
p110γ/p85
WT
shSCR2
shp110γ1
shp110γ2
Number of colonies in soft agar
C
Capan-1
BxPC-3
Panc-1
MIA PaCa-2
Treatment
pan-inh
α-inh
β-inh
γ-inh
δ-inh
FBS
pAkt (S473)
pAkt (T308)
Akt
pPRAS40 (T246)
Actin
D
Capan-1
BxPC-3
Panc-1
MIA PaCa-2
-FBS
OD
D1
D2
D3
D6

Figure 5

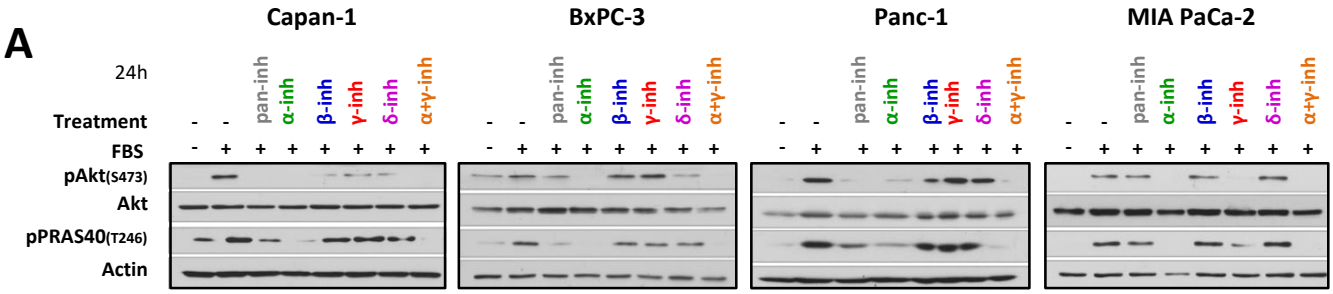
A
Capan-1
BxPC-3
Panc-1
MIA PaCa-2
24h
Treatment
pan-inh
α-inh
β-inh
γ-inh
δ-inh
α+γ-inh
FBS
pAkt(S473)
Akt
pPRAS40(T246)
Actin

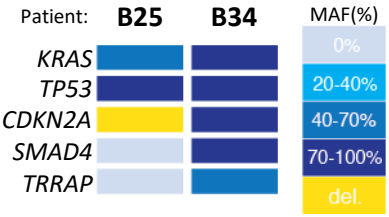
B
Patient:
B25
B34
MAF(%)
KRAS
TP53
CDKN2A
SMAD4
TRRAP
0%
20-40%
40-70%
70-100%
del.

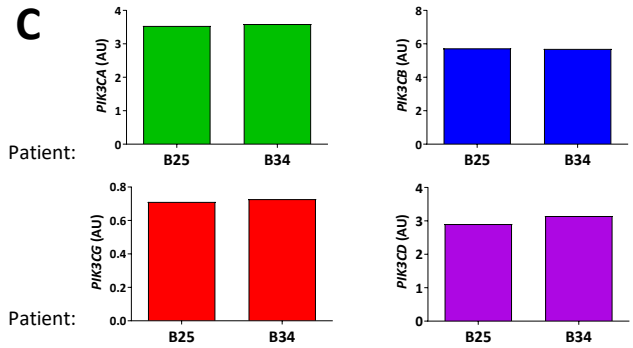
C
Patient:
PIK3CA (AU)
PIK3CB (AU)
PIK3CG (AU)
PIK3CD (AU)
B25
B34

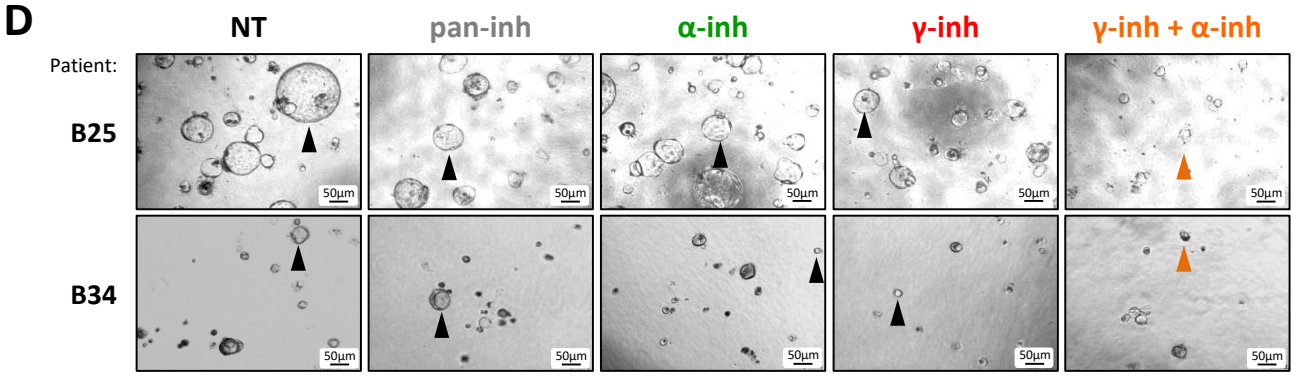
D
NT
pan-inh
α-inh
γ-inh
γ-inh + α-inh
Patient:
B25
B34
50µm

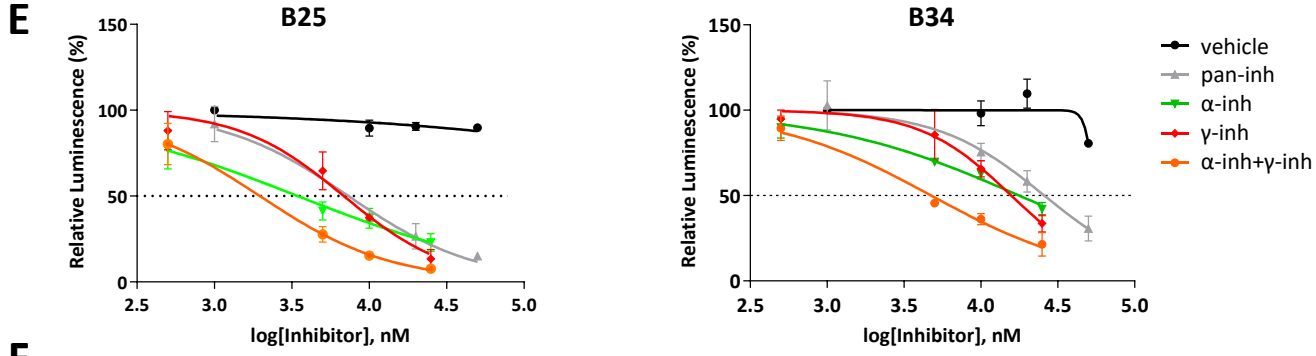
E
B25
B34
Relative Luminescence (%)
log[Inhibitor], nM
vehicle
pan-inh
α-inh
γ-inh
α-inh+γ-inh

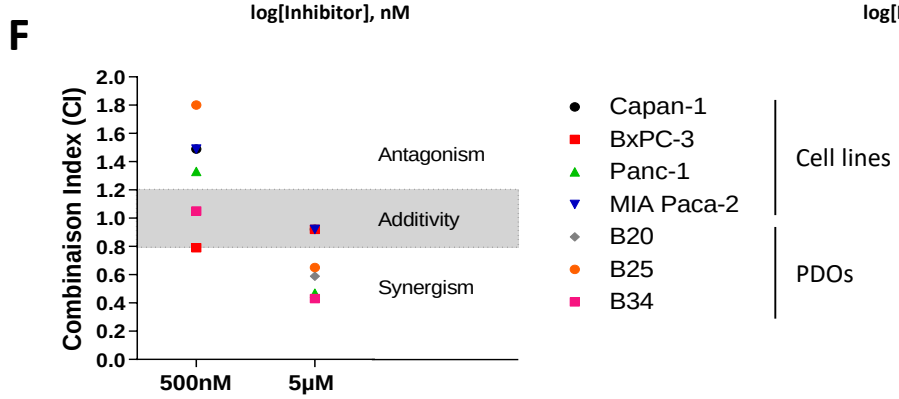
F
Combinaison Index (CI)
Antagonism
Additivity
Synergism
500nM
5µM
Capan-1
BxPC-3
Panc-1
MIA Paca-2
B20
B25
B34
Cell lines
PDOs